Kinematically complete measurement of the $\pi^+ d \rightarrow \pi^0 pp$ charge-exchange reaction

R. Tacik,* E. T. Boschitz, W. Gyles, C. R. Ottermann, M. Wessler, and U. Wiedner
Kernforschungszentrum Karlsruhe, Institut für Kernphysik and Institut für Experimentelle Kernphysik der Universität Karlsruhe, 7500 Karlsruhe, Federal Republic of Germany

H. Garcilazo
Institut für Theoretische Physik, Universität Hannover, 3000 Hannover, Federal Republic of Germany

R. R. Johnson
TRIUMF, 4004 Wesbrook Mall, Vancouver, British Columbia, Canada V6T 2A3
(Received 25 January 1990)

The triple differential cross section $d^3\sigma/d\Omega_{p_1} d\Omega_{p_2} dp_{p_1}$ was measured for the $\pi^+ d \rightarrow \pi^0 pp$ reaction as a function of proton momentum, in a kinematically complete experiment at $T_\pi = 228$ and 294 MeV. The two outgoing protons were detected in coincidence with plastic scintillator detectors, and their momenta determined by time-of-flight, at several angle pairs in regions of phase space far away from quasifree kinematics. The data are compared with predictions from the relativistic Faddeev calculation of Garcilazo.

I. INTRODUCTION

The systematic experimental investigation of the πNN system is very important in intermediate energy physics because its various reaction channels can in principle be calculated exactly using the relativistic Faddeev formalism and the known properties of the pion-nucleon and nucleon-nucleon subsystems. During the past few years remarkable theoretical progress on this system has been achieved.[1] Several theory groups have refined their calculations to the extent that a detailed comparison, even with sensitive polarization observables, on reactions with low cross sections, is possible. Moreover, it has been recognized that, for a stringent test, the comparison between theory and experiment must be extended to data from as many reaction channels as possible. With this purpose in mind, the present collaboration has studied the πd system for many years.

In order of decreasing cross section, the most important hadronic reaction channels are

$$\begin{aligned} \pi^\pm d &\rightarrow \pi^\pm NN \quad \text{(breakup)} \\ &\rightarrow \pi^\pm d \quad \text{(elastic)} \\ &\rightarrow \pi^0 NN \quad \text{(charge exchange)} \\ &\rightarrow NN \quad \text{(absorption)} \end{aligned}$$

A large amount of data has been accumulated on cross sections and polarization observables for the breakup,[2–6] elastic scattering[7–11] and absorption reactions.[12–14] By contrast, the charge exchange reaction has been neglected thus far. Rogers and Lederman[15] measured the total and differential $\pi^+ d \rightarrow \pi^0 pp$ cross sections at 85 MeV with a diffusion cloud chamber. They determined the charge exchange cross section $\sigma_{CX} = 12.2 \pm 2.2$ mb, and presented an angular distribution consisting of few data points with large uncertainties. Pewitt *et al.*[16] measured the cross sections for producing neutral products $(2n, 2n+\gamma, 2n+\pi^0)$ from $\pi^- d$ interactions at 142 MeV in a bubble chamber. After subtracting the absorption and radiative absorption cross sections from σ_{neutral}, the charge exchange cross section was found to be $\sigma_{CS} = 26.5 \pm 3$ mb at this energy. The most advanced bubble chamber experiment was performed by Norem,[17] who investigated the $\pi^+ d$ interaction at $T_\pi = 182$ MeV, taking 85 000 pictures. This relatively large number allowed him to determine cross sections for all four reaction channels with much better statistical accuracy than before. The total cross section was determined to be $\sigma_{CX} = 32.5 \pm 3$ mb. He also presented the first charge exchange differential cross sections with reasonable accuracy in the angular range up to 120°. The only more recent work was that of Moinester *et al.*,[18] who measured the differential cross section for the $\pi^+ d \rightarrow \pi^0 pp$ reaction at $T_\pi = 164$ MeV in the angular range between 5° and 165° using the LAMPF π^0 spectrometer. In the range beyond 35°, $d\sigma/d\Omega$ is comparable to the $\pi^- p \rightarrow \pi^0 n$ differential cross section, indicating dominance of the quasifree process. At very forward angles (small momentum transfer) the cross section drops to zero. The relativistic Faddeev calculation of Garcilazo reproduces the data quite well over the full angular range (see Ref. 19). In order to put the Faddeev theory to a more stringent test in this reaction channel a kinematically complete measurement would be desirable, and that was the purpose of the present experiment.

In order to perform a kinematically complete experiment for the $\pi d \rightarrow \pi^0 NN$ reaction, one has to measure five of the nine possible final state variables, for example, the polar and azimuthal angles of two of the three particles, and the momentum of one of them. Because of the complications involved in detecting neutral particles, we

have elected to study the $\pi^+ d \rightarrow \pi^0 pp$ reaction, and detect the two outgoing protons in coincidence. We have measured the energies of both protons, which means that we are actually kinematically overdetermined, and can use this fact to suppress background. There is also a physics advantage to our choice: Except for the extreme momentum regions (where one of the protons has a small momentum), the kinematical regions away from the quasifree charge exchange process ($\pi^+ n \rightarrow \pi^0 p$) are explored. As we have learned from our studies of the $\pi^+ d \rightarrow \pi^+ pn$ reaction, the regions away from quasifree kinematics are the physically more interesting ones.

II. EXPERIMENTAL PROCEDURE

The experiment was performed in the $\pi M1$ area of the Paul Scherrer Institute (formerly SIN) in Switzerland. The experimental setup is shown in Fig. 1. Six proton detectors were used in the experiment. Each of them consisted of a thin plastic scintillator (a) ($0.5 \times 20.0 \times 70.0$ cm^3) at a distance of 1.88 m from the center of the liquid deuterium target, and a thick counter (b) ($20.0 \times 20.0 \times 70.0$ cm^3) 12 cm behind counter (a). Each of the (a) and (b) counters was viewed by two photomultipliers, one at either end. The electronics were set up to detect a coincidence between any one of the three detectors on the right side of the beam with any one of the three detectors on the left side of the beam. In order to keep the energy threshold as low as possible, only the (a) counters were in the hardware trigger, although ADC and TDC information was recorded for both (a) and (b) counters for every event. Proton momenta were determined from their times-of-flight, calibrated using the $\pi^+ p \rightarrow \pi^+ p$ reaction, at a number of angles, with a solid piece of CH_2 in place of the liquid deuterium target.

The experiment was performed at two incident pion energies, $T_\pi = 228$ and 294 MeV. Typical incident fluxes at these two energies were 6.5 and 8.0 MHz. The incident pions were detected by a scintillation counter hodoscope $S1$ and a beam defining counter $S2$. The hodoscope consisted of five scintillation strips ($0.2 \times 1.0 \times 10.0$ cm^3) and was placed 1.5 m upstream from the target. The beam defining counter with a 3 cm diameter hole in the center was operated as veto counter. A beam event was defined by BEAM$= S1 \cdot \bar{S}2 \cdot$rf where rf is a radio frequency pickup signal from the accelerator. For a continuous stability check of the position, shape, and intensity of the pion beam, two types of monitors were used: a 10 cm $\times$ 10 cm multiwire chamber as a beam profile monitor and a set of scintillation counters $M1-M3$. The profile monitor with an integrating readout was connected to an oscilloscope on which the X and Y profile of the beam was continuously displayed. The scintillation counters $M1-M3$ were arranged as a triple counter telescope and viewed the hodoscope $S1$ from an angle above the scattering plane.

The liquid deuterium target cell was disc shaped, 2.5 cm thick, and 10.6 cm in diameter, oriented at 0° with respect to the incident beam. Deuterium gas ballast chambers on both sides of the cell separated the liquid target from the vacuum. The 36 μm Mylar foils of the target walls were prestretched. In a separate experiment it was shown that the deformation of the foils due to hydrostatic pressure of the liquid deuterium was negligible. The target cell could easily be evacuated in order to allow for background measurements.

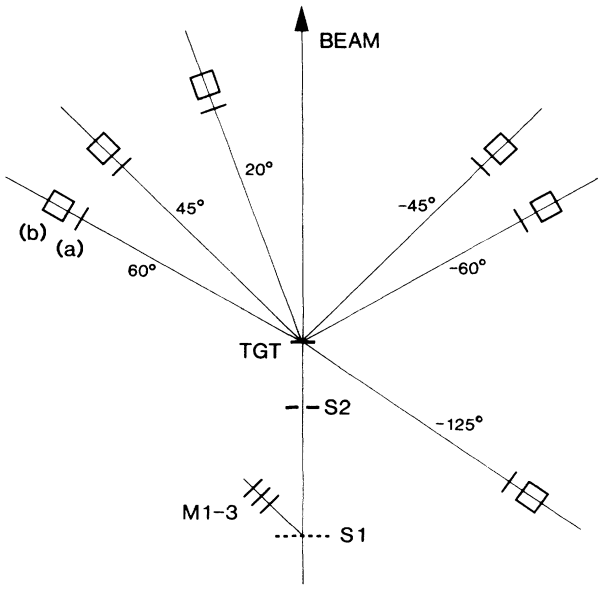

FIG. 1. Schematic drawing of the experimental setup.

III. DATA REDUCTION

The first step in the data reduction procedure involved making particle identification cuts in order to reduce background from reactions such as $\pi^+ d \rightarrow \pi^+ pn$. This was accomplished by constructing polygons around the proton bands in two-dimensional histograms of time-of-flight (TOF) versus pulse height for each counter. Note that a possibility of misidentification occurred for a few lower energy pions which did not pass through counter (b) as these could not be clearly distinguished from high energy protons.

Next, the measured times-of-flight were corrected for energy loss in the target and surrounding material, and two-dimensional histograms of TOF_1 vs TOF_2 were constructed. A typical plot is shown in Fig. 2 for the counter combination (60°, −45°) at $T_\pi = 294$ MeV. Also shown in Fig. 2 are the kinematic loci along which particles from the $\pi^+ d \rightarrow \pi^0 pp$, $\pi^+ d \rightarrow \gamma pp$, and $\pi^+ d \rightarrow \pi^+ pn$ reactions are expected to lie. An enhancement around the $\pi^+ d \rightarrow \pi^0 pp$ locus is evident. It must be noted, however, that our TOF resolution is not good enough to separate events from the $\pi^+ d \rightarrow \gamma pp$ radiative absorption channel. Although it is reasonable to expect the total cross section for electromagnetic interactions to be smaller than the total cross section for strong interactions by two orders of magnitude, this is not necessarily the case in the present experiment, where we are measuring far away from quasifree kinematics. Nevertheless, we have assumed the radiative absorption cross section to be negligible in the present analysis.

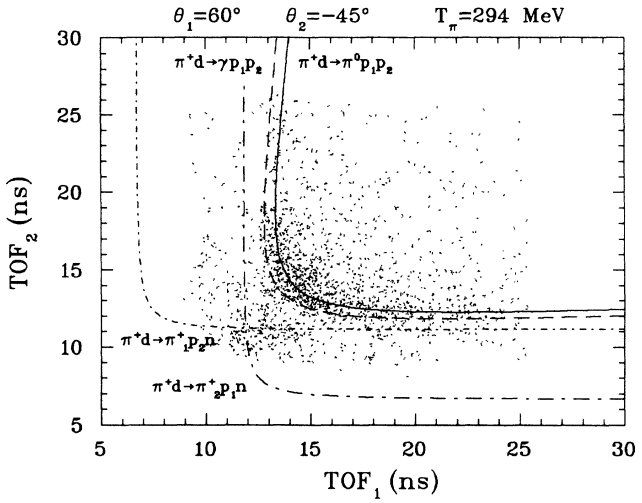

FIG. 2. Density plot of TOF_1 vs TOF_2 (measured with the full target). The various lines represent kinematic loci along which events from the indicated reactions would be expected to lie.

In Fig. 3(a) we show a histogram of the shortest distance (in ns) between measured TOF_1 and TOF_2 times and the kinematic locus for the $\pi^+ d \to \pi^0 pp$ reaction, for both full-target and background runs. Positive values correspond to measured events above or to the right of the locus, while negative values correspond to events below or to the left. The slight mismatch at the ends of the spectrum is due to the different energy losses in the full and empty targets. The difference between full-target and background runs is shown in Fig. 3(b). Events outside the region indicated by the two vertical lines were rejected from further analysis. Note that the difference spectrum goes cleanly to zero to the right of the main peak. The small peak to the left of the main one, which is due to misidentified pions from the $\pi^+ d \to \pi^+ pn$ reaction, is thus easily eliminated. Note also that the main peak is slightly asymmetric and its width is somewhat larger than our 1 ns timing resolution. This is due to the fact that we have averaged the data over the full vertical acceptance of the counters.

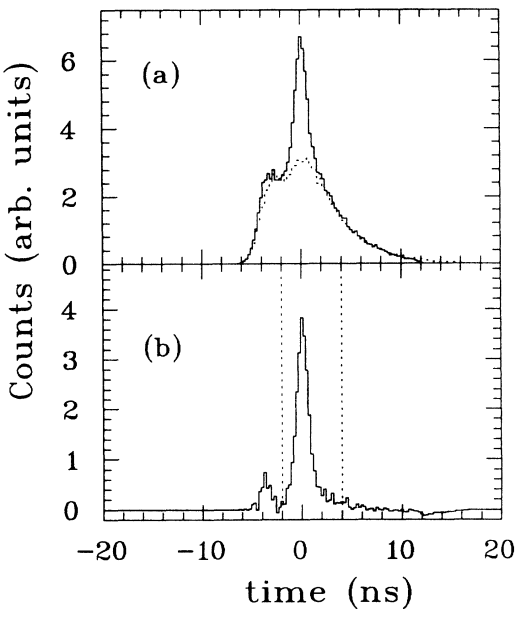

FIG. 3. Distance of scattering events from the locus for the $\pi^+ d \to \pi^0 pp$ reaction for the angle pair (60°, −45°) at $T_\pi = 294$ MeV. In (a), the dotted line represents data taken with an empty target, the solid line with the target full. The distribution in (b) is the difference.

In the final step of the data reduction procedure, the yield of protons in a given momentum bin was determined, and the triple differential cross section calculated from

$$\frac{d^3\sigma}{d\Omega_{p_1} d\Omega_{p_2} dp_{p_1}} = \frac{\text{Yield}}{N_{\text{beam}} N_{\text{tgt}} \epsilon \Delta\Omega_{p_1} \Delta\Omega_{p_2} \Delta p_{p_1}} ,$$

where N_{beam} is the number of incident pions, N_{tgt} is the number of deuterons per cm^2 in the target, ϵ is the efficiency of the data acquisition system measured during the experiment (0.7–0.8), $\Delta\Omega_{p_1}$ and $\Delta\Omega_{p_2}$ are the proton solid angles (39.8 msr), and Δp_{p_1} is the proton momentum bin (20 MeV/c).

Systematic uncertainties in the measurement of the cross section arise from uncertainties in the determination of the target thickness, in the solid angles of the detectors, and in the incident beam intensity, as well as effects associated with background subtraction. The overall systematic error is estimated to be 15%, and is not included in the statistical uncertainties presented in the figures in the next section.

Note that there are some instances where there are two values of p_2 corresponding to a given value of p_1. In all cases, we have only taken one solution. In order to clari-

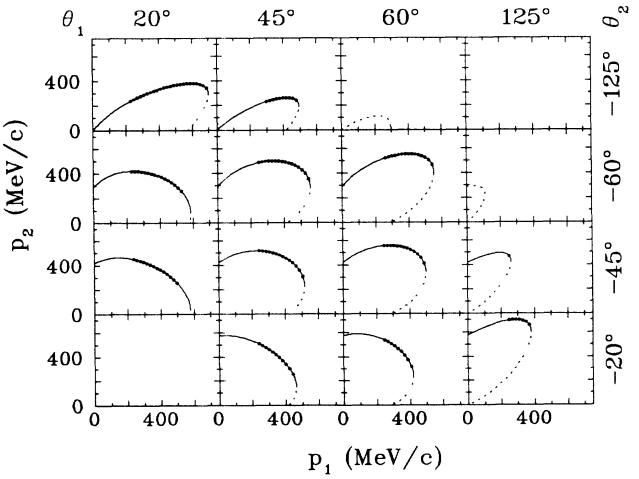

FIG. 4. Kinematics for all possible counter combinations in the present experiment. The solid lines represent the range of the calculations, and the points correspond to the momentum bins for which data are presented.

fy this point, and provide information for the discussion in the next section, we show in Fig. 4 the full kinematics, at $T_\pi = 294$ MeV, for our counter configuration. The solid line corresponds to the range of the calculations to be presented, and the points to the momentum bins for which we present data.

IV. THEORY

The theoretical predictions presented in the next section are the results of a relativistic three-body Faddeev calculation, using the spectator-on-mass-shell approximation, which has been described in detail in Ref. 20. The same approach has been used with considerable success in the calculation of the normal breakup ($\pi^+ d \to \pi^+ pn$) reaction (see Ref. 5).

The spectator-on-mass-shell approach solves the relativistic version of the Faddeev equations by imposing the condition that all the spectator particles in the initial, final, and intermediate state be put on the mass shell, and by introducing an isobar ansatz for the two-body amplitudes (like the delta isobars corresponding to the pion-nucleon P_{33} channel shown in Fig. 5). The input of the

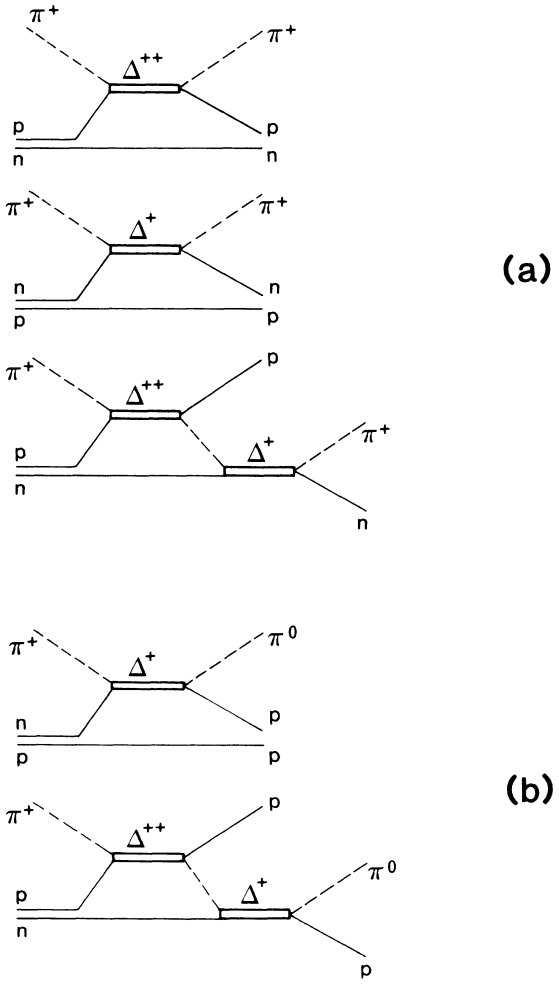

FIG. 5. (a) Main diagrams contributing to the $\pi^+ d \to \pi^+ pn$ reaction. (b) Main diagrams contributing to the $\pi^+ d \to \pi^0 pp$ reaction.

equations are the six S- and P-wave pion-nucleon channels S_{11}, S_{31}, P_{11}, P_{13}, P_{31}, and P_{33}, and the nucleon-nucleon channels $^1S_0$ and $^3S_1$-$^3D_1$. The two-body amplitudes for the πN channels are constructed directly from the experimental phase shifts and are extrapolated off-shell by multiplying by the monopole form factor $(\beta^2+p_0^2)/(\beta^2+p^2)$ for the particle that is going off-shell, where p is the magnitude of the πN relative three momentum, and the cutoff parameter $\beta = 600$ MeV/c. The nucleon-nucleon channels are constructed similarly of separable form such that they would agree with the bound-state solution of the Paris potential for the $^3S_1$-$^3D_1$ channel and the corresponding anti-bound-state solution for the $^1S_0$ channel. The integral equations are solved along the real axis using the method of Padé approximants by integrating over the logarithmic singularities and discontinuities of the kernels with a variable Gauss mesh of between 34 and 54 points which gives solutions with an estimated accuracy of $\sim 1\%$.

Pion deuteron elastic and inelastic scattering is described by the operator

$$T = T_2 + T_3 \ , \tag{1}$$

where the amplitudes T_i are the solutions of the Faddeev equations

$$T_i = (1-\delta_{il})t_i + \sum_{j \neq i} t_i G_0 T_j; \quad i,j = 1,2,3 \ , \tag{2}$$

and we have assumed that particle 1 is the pion and particles 2 and 3 the two nucleons. The elastic scattering amplitude is obtained by taking the matrix elements of the operator (1) between initial and final deuteron wave functions and plane-wave pions, that is,

$$T_{\pi d \to \pi d} = \langle \mathbf{k}'_\pi \phi_d | T | \mathbf{k}_\pi \phi_d \rangle \ . \tag{3}$$

The breakup and charge-exchange amplitudes are obtained by taking the matrix elements of the operator (1) between initial deuteron wave function and plane-wave pion and final nucleon-nucleon continuum wave function and the corresponding plane-wave pion, that is,

$$T_{\pi d \to \pi NN} = \langle \mathbf{k}'_\pi \chi^{(-)}_{NN} | T | \mathbf{k}_\pi \phi_d \rangle \ . \tag{4}$$

Thus, the elastic, breakup, and charge-exchange amplitudes are described by the same operator T except that the two nucleons in the final state are in one case in a bound state and in the other two cases in continuum states. The breakup and charge-exchange reactions differ from each other only in the fact that they have different isospin structure in the nucleon-nucleon final-state wave function. Since the isospin of the deuteron is equal to 0, the total isospin of the system is equal to 1, so that in the case of the normal breakup reaction, the cross section is the sum of two terms corresponding to the nucleon-nucleon pair having isospin 0 and 1. The charge-exchange cross section, however, is given only by the term with isospin 1. Thus, the dominant nucleon-nucleon $^3S_1$ final-state interaction is forbidden in this channel, and only the weak $^1S_0$ final-state interaction enters (the $^3S_1$-$^3D_1$ channel contributes of course in the intermediate states).

The operator T defined by Eqs. (1) and (2) can be written in the multiple scattering from

$$T=t_2+t_3+t_2G_0t_3+t_3G_0t_2+\cdots , \tag{5}$$

so that in the case of the normal breakup, the single-scattering terms t_2 and t_3 give rise to the first two graphs of Fig. 5(a), the term $t_2G_0t_3$ to the third graph, etc., if one takes for the nucleon-nucleon continuum wave function only the plane-wave part. Notice that while both proton and neutron diagrams contribute in lowest order to the normal breakup, in the case of the charge-exchange reaction depicted in Fig. 5(b) only the neutron exchange graph contributes in lowest order. However, since we are using the isospin formalism where the two nucleons are identical particles, the amplitude for the charge-exchange process is equal to $\sqrt{2}$ times the normal breakup amplitude with the two nucleons in the isospin one state. Thus, one still has to take both terms t_2 and t_3 since this ensures that the amplitude be correctly antisymmetrized with respect to the exchange of the two final protons as required by the Pauli principle, that is, the graph arising from t_3 is precisely the exchange graph from t_2. The same result holds of course to all orders.

V. RESULTS AND DISCUSSION

We present our results for all possible counter combinations at $T_\pi=228$ and 294 MeV in Figs. 6 and 7, respectively. There were no counters positioned to measure the combinations (20°, −20°) and (125°, −125°), and the proton momenta for the combinations (125°, −60°) and (60°, −125°) were below our experimental thresholds. Note that for two counter combinations, (45°, −45°) and (60°, −60°), the same cross section was measured twice, and that a similar situation occurred for the combinations (45°, −60°) and (60°, −45°). In each case we had two independent measurements of the same cross section. In each case the data were in good agreement and the plotted values represent the averages of the two measurements. The solid lines in Figs. 6 and 7 represent the results of a full three-body Faddeev calculation from one of us (H.G.). In general, there is remarkably good agreement, considering that the calculations in fact constitute predictions and have not in any way been scaled or adjusted to fit the data. The dotted lines in Figs. 6 and 7 represent the three-body phase space:

$$\frac{d^3R}{d\Omega_{p_1}d\Omega_{p_2}dp_{p_1}}=\frac{|T|^2}{(2\pi)^3}\int\frac{p_{p_1}^2p_{p_2}^2}{E_{p_1}E_{p_2}E_{\pi^0}}dp_{p_2}\times\delta(E_T-E_{p_1}-E_{p_2}-E_{\pi^0}) ,$$

with $|T|^2$ set equal to 1.0 at 294 MeV and 3.0 at 228 MeV. It is evident that for many of the angle combinations at larger proton momenta the data are described equally well by the phase space and the full calculation, indicating a constant matrix element. There are some exceptions, however. For the combination (60°, −60°), for example, the decrease of the data with increasing proton momentum is described much better by the full calculation than by the smoothly increasing phase space. The same is true to a lesser extent for the combination (20°, −125°).

For all of the angle combinations, the data show a large increase for the largest proton momenta, which is predicted by the full calculation. Although the phase space also increases in this range, it actually drops right at the end, and so the good agreement between the predictions and that data must be attributed to a genuine physics effect.

The most significant differences between the full calculation and the phase space occur at the lowest proton momenta, where the phase space is always decreasing while the full calculation is generally rising. This rise must be attributed to the increased importance of the quasifree process, $\pi^+n\rightarrow\pi^0p_2$, with p_1 acting as a spectator at low momenta. It is interesting to note that for the two angle combinations (20°, −60°) and (20°, −45°) a similar situation occurs for large p_1 momenta. That is, the quasifree process $\pi^+n\rightarrow\pi^0p_1$ with p_2 acting as a spectator be-

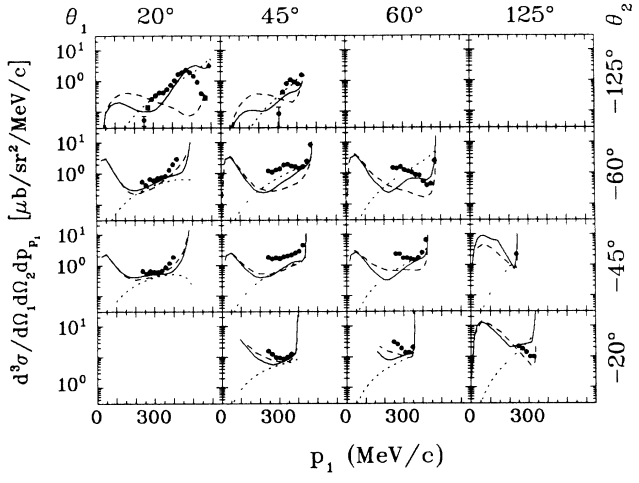

FIG. 6. Triple differential cross sections obtained at $T_\pi=228$ MeV. The solid line represents the theoretical prediction from Garcilazo (full calculation), the dotted line is the phase space, and the dashed line is the impulse approximation.

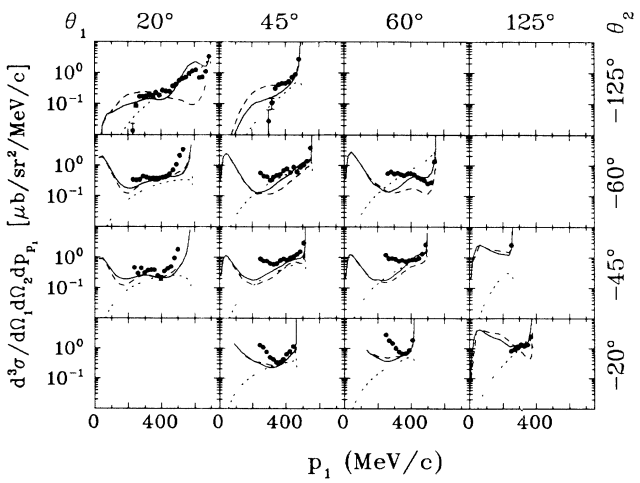

FIG. 7. Same as Fig. 6 for $T_\pi=294$ MeV.

comes important. The special kinematics for these two angle combinations should be clear from inspection of Fig. 4. It is evident from Figs. 6 and 7, however, that in general the data rise even more quickly than the full calculation in these momentum ranges. It is interesting to speculate at this point whether the underprediction of the data is caused by an underestimation of the strength of the quasifree process, or whether it is caused by some interference between the quasifree and higher-order contributions. In order to shed some light on this question we also show as the dashed line in Figs. 6 and 7 the results of an impulse approximation, calculation, that is, the calculation with only the quasifree contribution, ignoring all the higher-order terms. It is evident that for many angle combinations, most notably (20°, −125°), (45°, −125°), (60°, −60°), and (125°, −20°), there are significant differences between the full calculation and the impulse approximation, especially at larger proton momenta. In these regions, the full calculation provides a better description of the data, indicating the importance of higher-order processes. At lower values of proton momenta, however, closer to quasifree kinematics, there is little difference between the full calculation and the impulse approximation. It is thus still not evident why the low momentum data are underpredicted. This may be due to (i) the deuteron wave function used in the calculation (one may, for example, consider variations in the inner part of the deuteron wave function like the ones proposed by Certov, Mathelitsch, and Moravcski[21]), (ii) neglecting higher-order contributions such as the residual $N\Delta$ interaction proposed by Andrade, Ferreira, and Dosch[22] (arising, for example, from the exchange of a ρ meson or from a direct $\pi\Delta\Delta$ vertex), or (iii) effects of the $(\pi,2\pi)$ reaction channel which is only partially included in the present calculation through the π-nucleon input.

The first two possibilities call for further theoretical investigation, while the last might possibly be addressed by repeating the present experiment at a lower incident pion energy, although it is evident from the present data that there is no strong energy dependence in the measured results. Some notable differences are a sharper rise at 294 MeV than at 228 MeV at lower proton momenta for the angle combinations (45°, −20°) and (60°, −20°). The dip at larger momenta for the angular combinations (20°, −125°) and (60°, −60°) is much more pronounced at 228 MeV, and the similar dip for (45°, −125°) that is seen at 228 MeV is no longer apparent at 294 MeV. Finally, the cross section for (125°, −20°) increases at 294 MeV, and decreases at 228. These differences do not seem to be well reproduced by the calculation. One interesting difference in the calculations at the two energies lies in the interference between the quasifree and higher-order contributions. For the angle combinations (45°, −45°), for example, at lower proton momenta, the interference is destructive at 228 MeV, and constructive at 294 MeV.

VI. SUMMARY AND OUTLOOK

The triple differential cross section $d^3\sigma/d\Omega_{p_1}d\Omega_{p_2}dp_{p_1}$ was measured for the $\pi^+d\rightarrow\pi^0pp$ reaction as a function of proton momentum, in a kinematically complete experiment at $T_\pi=228$ and 294 MeV. The two outgoing protons were detected in coincidence with plastic scintillator detectors, and their momenta determined by time-of-flight. The data were compared with predictions from the relativistic Faddeev calculation of Garcilazo. In general, good agreement was found at both incident pion energies. In the region of large proton momenta, the full calculation provided a better description of the data than the impulse approximation. At lower proton momenta, closer to quasifree kinematics, the experimental values were much higher than the calculations. Although we have speculated on some possible reasons for these discrepancies, more definite conclusions must await further investigations.

There are a number of reasons why and in what way this charge exchange reaction should be further investigated. From the data presented in Figs. 6 and 7 one recognizes a lower cutoff of the data near 200 MeV/c proton momentum. This cutoff is essentially given by the energy loss in the target. In order to extend the phase space of the reaction to lower nucleon momenta one would have to go to the charge symmetric reaction $\pi^-d\rightarrow\pi^0nn$. However, the advantage of a larger phase space may be paid for by a lower counting rate due to lower negative pion fluxes at the meson factories, and lower detection efficiency for neutrons.

An important extension of the present experiment would be the measurement of the analyzing power iT_{11} of the triple differential cross section $\sigma(\theta_{p_1},\theta_{p_2},p_{p_2})$ using a vector polarized deuteron target. From our earlier studies of iT_{11} in the πd breakup, elastic scattering, and absorption reactions it is clear that this observable puts the theory to a more severe test. Some typical predictions from Garcilazo for iT_{11} are shown in Fig. 8. Sizable analyzing power is seen in some regions of phase space.

The $\pi^+d\rightarrow\pi^0pp$ reaction may also be interesting in other respects. Since in the charge-exchange reaction $\pi^+d\rightarrow\pi^0pp$ and $\pi^-d\rightarrow\pi^0nn$ the dominant nucleon-

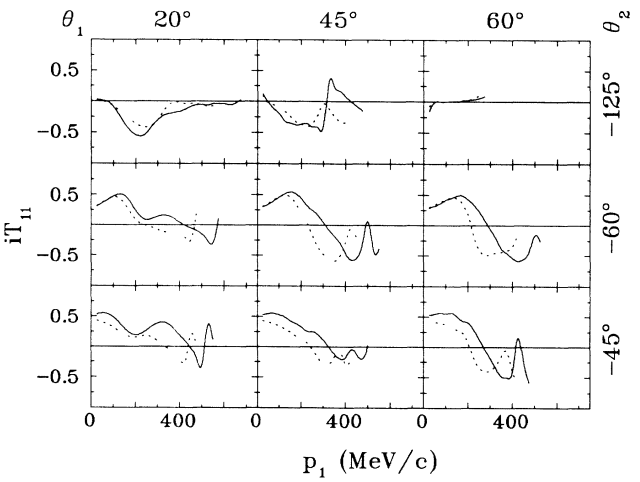

FIG. 8. Predictions for the analyzing power iT_{11} for some proton-proton angle pairs. The solid line is for $T_\pi=294$ MeV, the dashed line for 228 MeV.

nucleon $^3S_1$ final-state interaction is forbidden by the Pauli principle, only the weak $^1S_0$ final-state interaction (see Ref. 5) and the pion-nucleon interactions enter, so that these reactions may be very well suited to study the quasi-two-body reactions $\pi^+ d \to p\Delta^+$ and $\pi^- d \to n\Delta^0$ in order to isolate the effects of the residual short-range N-Δ interaction.

The existence of dibaryon resonances is still an open question (for a critical review see Ref. 23). There is general consensus that the most reliable way to discover such exotics would be to detect narrow structures in the excitation function of invariant mass distributions. Recently, a narrow enhancement in the pp invariant mass distribution ($\Gamma < 5$ MeV/c^2) has been observed at 2.014 GeV/c^2 in the $\gamma d \to \pi^- pp$ reaction.[24] The significance of this enhancement is 4.7 standard deviations. Although the location of this structure is close to the total $(pp\pi^-)$ mass, and therefore some threshold effects cannot be ruled out, the narrow width may be indicative of a dibaryon signal. This result should be confirmed by an independent experiment, e.g., the study of the $\pi^+ d \to \pi^0 pp$ reaction in that pp mass range.

ACKNOWLEDGMENTS

We would like to thank R. Meier and S. Ritt for their help in replaying the data. This work would have been impossible without the generous help and considerable skills of the staff of the Paul Scherrer Institute. It was supported by the Bundesministerium für Forschung und Technologie of the Federal Republic of Germany.

*Present address: Department of Physics, University of Regina, Regina, Saskatchewan, Canada S4S 0A2.

[1]H. Garcilazo and T. Mizutani, Few-Body Syst. **5**, 127 (1988).
[2]E. L. Mathie, G. R. Smith, E. T. Boschitz, W. Gyles, C. R. Ottermann, S. Mango, J. A. Konter, A. Matsuyama, R. R. Johnson, and R. Olszewski, Phys. Lett. **154B**, 28 (1985).
[3]W. Gyles, E. T. Boschitz, H. Garcilazo, W. List, E. L. Mathie, C. R. Ottermann, G. R. Smith, R. Tacik, and R. R. Johnson, Phys. Rev. C **33**, 583 (1986).
[4]W. Gyles, E. T. Boschitz, H. Garcilazo, E. L. Mathie, C. R. Ottermann, G. R. Smith, S. Mango, J. A. Konter, and R. R. Johnson, Phys. Rev. C **33**, 595 (1986).
[5]W. List, E. T. Boschitz, H. Garcilazo, W. Gyles, C. R. Ottermann, R. Tacik, M. Wessler, U. Wiedner, and R. R. Johnson, Phys. Rev. C **37**, 1587 (1988).
[6]W. List, E. T. Boschitz, H. Garcilazo, W. Gyles, C. R. Ottermann, R. Tacik, S. Mango, J. A. Konter, B. van den Brandt, and G. R. Smith, Phys. Rev. C **37**, 1594 (1988).
[7]G. R. Smith, E. L. Mathie, E. T. Boschitz, C. R. Ottermann, S. Mango, J. A. Konter, M. Daum, M. Meyer, R. Olszewski, and F. Vogler, Phys. Rev. C **29**, 2206 (1984).
[8]C. R. Ottermann, E. T. Boschitz, W. Gyles, W. List, R. Tacik, R. R. Johnson, G. R. Smith, and E. L. Mathie, Phys. Rev. C **32**, 928 (1985).
[9]C. R. Ottermann, E. T. Boschitz, W. Gyles, W. List, R. Tacik, M. Wessler, S. Mango, B. van den Brandt, J. A. Konter, D. R. Gill, and G. R. Smith, Phys. Rev. C **38**, 2296 (1988).
[10]C. R. Ottermann, E. T. Boschitz, H. Garcilazo, W. Gyles, W. List, R. Tacik, M. Wessler, S. Mango, B. van den Brandt, J. A. Konter, and E. L. Mathie, Phys. Rev. C **38**, 2310 (1988).
[11]H. Garcilazo, E. T. Boschitz, W. Gyles, W. List, C. R. Ottermann, R. Tacik, and M. Wessler, Phys. Rev. C **39**, 942 (1989).
[12]E. L. Mathie, G. R. Smith, E. Boschitz, J. Hoftiezer, and M. Meyer, Z. Phys. A **313**, 105 (1983).
[13]G. R. Smith, E. L. Mathie, E. T. Boschitz, C. R. Ottermann, W. Gyles, W. List, S. Mango, J. A. Konter, B. van den Brandt, R. Olszewski, and R. R. Johnson, Phys. Rev. C **30**, 980 (1984).
[14]C. R. Ottermann, E. T. Boschitz, W. Gyles, W. List, R. Tacik, S. Mango, J. A. Konter, B. van den Brandt, and G. R. Smith, Phys. Rev. C **33**, 1802 (1986).
[15]K. C. Rogers and L. M. Lederman, Phys. Rev. **105**, 247 (1957).
[16]E. G. Pewitt, T. H. Fields, G. B. Yodh, J. G. Fetkovich, and M. Derrick, Phys. Rev. **131**, 1826 (1963).
[17]J. H. Norem, Nucl. Phys. **B33**, 512 (1971).
[18]M. A. Moinester, A. Erell, E. Piasetsky, J. Alster, J. D. Bowman, H. W. Baer, M. D. Cooper, F. Irom, U. Sennhausser, H. Ziock, and M. Leach, XI International Conference on Particle and Nuclei, Kyoto, 1987, Abstract Book I (unpublished).
[19]E. T. Boschitz, in *Pion-Nucleus Physics: Future Directions and New Facilities at LAMPF*, Proceedings of the Los Alamos Conference on Pion-Nucleus Physics, AIP Conf. Proc. No. 163, edited by R. J. Peterson and D. D. Strottman (AIP, New York, 1987), p. 2.
[20]H. Garcilzao, Phys. Rev. C **35**, 1804 (1987).
[21]A. Certov, L. Mathelitsch, and M. J. Moravcsik, Phys. Rev. C **36**, 2040 (1987).
[22]S. C. B. Andrade, E. Ferreira, and H. G. Dosch, Phys. Rev. C **34**, 226 (1986).
[23]M. P. Locher and A. Svarc, J. Phys. G **11**, 183 (1985).
[24]B. Bock, W. Ruhm, K. H. Althoff, G. Anton, W. Ferber, H. W. Gelhausen, T. Jahnen, O. Kaul, D. Menze, W. Mayer, T. Miczaika, E. Roderburg, E. Schilling, E. Schenuit, D. Sundermann, and W. J. Schwille, Nucl. Phys. **A459**, 573 (1986).